Coupled Systems Mechanics, *Vol. 10, No. 3 (2021) 247-261*
DOI: https://doi.org/10.12989/csm.2021.10.3.247

On the finite element modeling of a particular shallow foundation system for soft soil

Soelarso Soelarso[1], Eduard Antaluca[1], Jean-Louis Batoz*[2] and Fabien Lamarque[1]

[1]*Laboratoire Roberval, Alliance Sorbonne Université-Université de Technologie de Compiègne, CS 60319, 60203 Compiègne Cedex, France*
[2]*Laboratoire Avenues, Alliance Sorbonne Université-Université de Technologie de Compiègne, CS 60319, 60203 Compiègne Cedex, France*

(Received April 14, 2021, Revised May 10, 2021, Accepted May 21, 2021)

Abstract. The presentation deals with an investigation on the static and dynamic behavior of a five floors reinforced concrete building supported by a shallow foundation system, called SNSF (Spider Net System Footing). The present study concentrates on the linear static under permanent and life vertical loads and on the free vibrations of the upper structure and the foundations. The study based on performing 3D solid finite elements includes the soil underneath (one layer of 2 m and an additional layer of 9 m). Several aspects are investigated like: the structural analysis of the SNSF foundation compared to a simpler raft foundation and the soil-foundation interaction of the soil and the structure-foundation system on the first frequencies and modes of vibration.

Keywords: shallow foundation system; finite element simulation; earthquake resistant; free vibration analysis; Altairworks

1. Introduction

The SNSF (Spider Net System Footing) system is an alternative shallow foundation system so far used more than one hundred times for the building construction in Indonesia (https://www.katama.co.id). The system is particularly adapted in poor soil conditions. That system is also used for specific road and landing runway constructions. The SNSF system is claimed to be economic compared to a traditional raft system but it has also been considered as earthquake resistant as the SNSF appears to act in a monolithic way with the upper structure with respect to soil structure interaction, so that limited damages (like differential settlements) are observed in earthquake conditions.

Figs. 1 and 2 present a 3D view of the economy building built between 2018 and 2020 on the UNTIRTA Campus project in the Banten province on Java island (Indonesia). That building is a typical RC (reinforced concrete building) 84 m length and 23 m width with 5 floors and two roofs. That building is fully supported by a SNSF foundation system with of 92 columns; 48 inside columns with a cross section of 0.6 m by 0.6 m. Fig. 3 shows the SNSF foundation (in red) and the upper structure (in brown). Fig. 4 shows a top view of the SNSF foundation under the horizontal

*Corresponding author, Professor, E-mail: jean-louis.batoz@utc.fr

http://www.techno-press.org/?journal=csm&subpage=8 ISSN: 2234-2184 (Print), 2234-2192 (Online)

Fig. 1 UNTIRTA Campus Project: 3d view

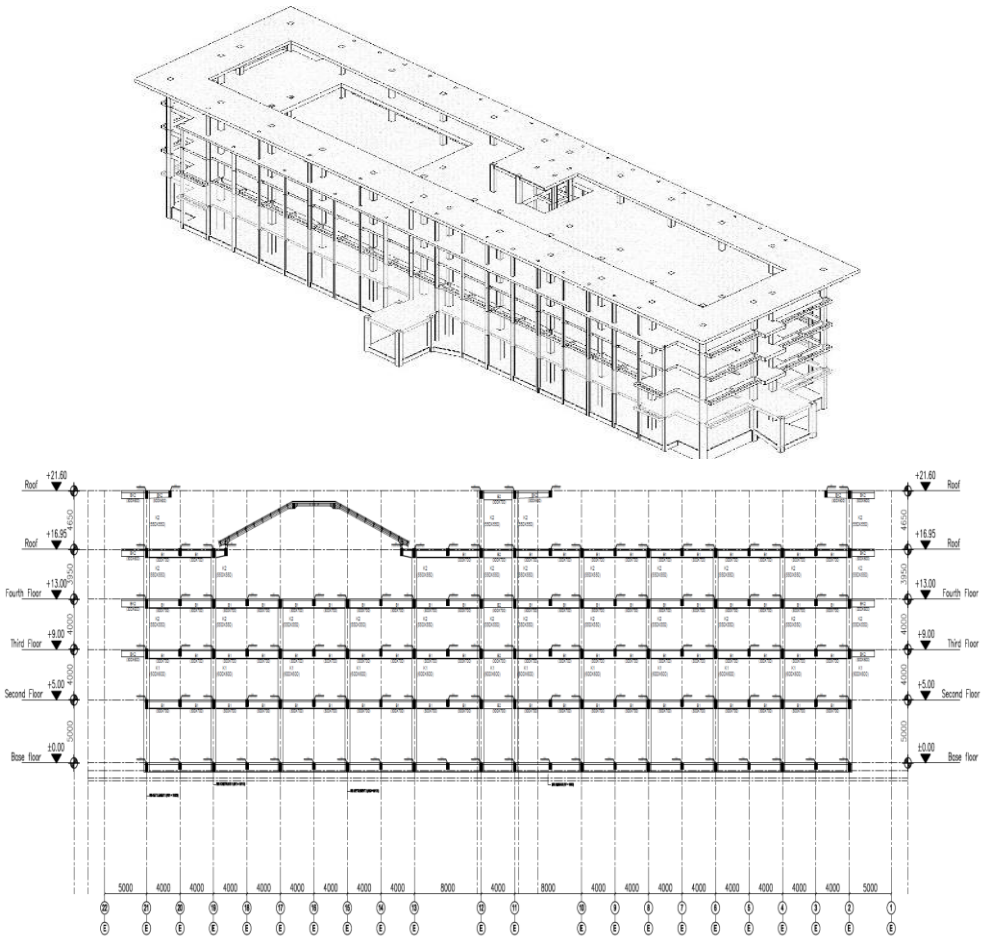

Fig. 2 Economy Building (3D view and cross section)

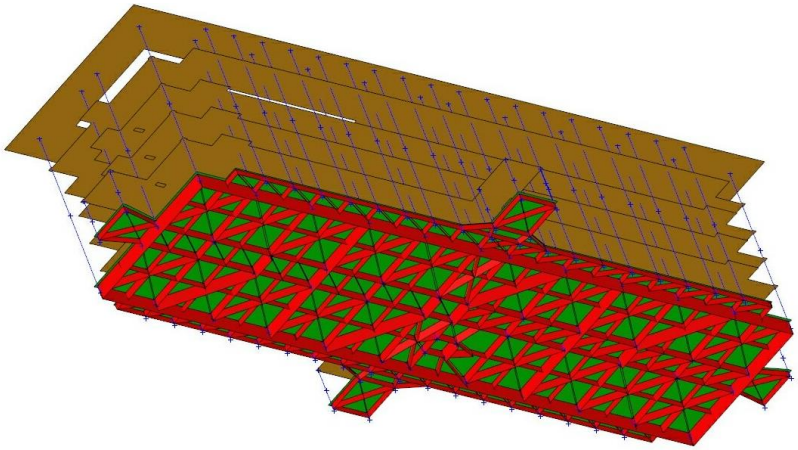

Fig. 3 3D view of building showing the upper structure and the SNSF foundation system (in red)

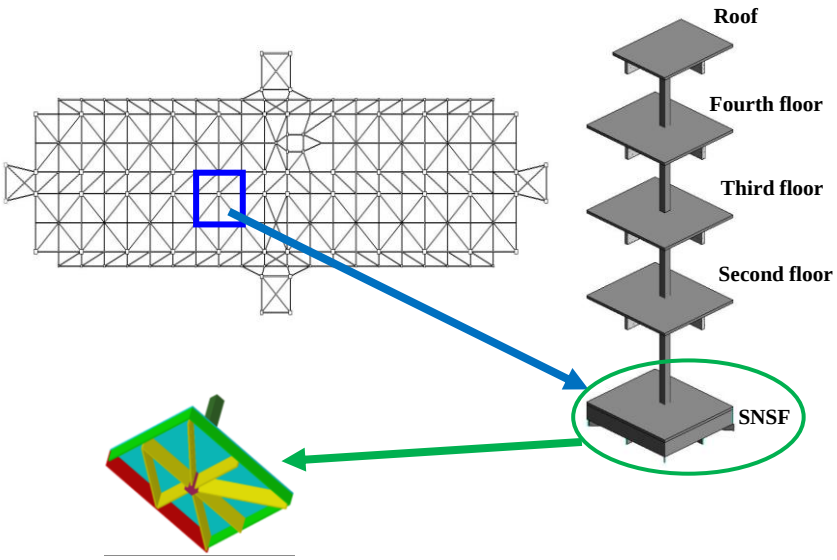

Fig. 4 Top view of the floor level and location of one SNSF cell

slab of the first floor. Fig. 4 also presents one cell of SNSF involving one column of 17 m total length with a square cross section (0.6 m×0.6 m) and four floors (first at 5 m from ground level, upper levels with 4 m height each). The chosen cell of dimensions 7 m by 8 m is extracted from the whole foundation system. The upper floors and roof involve orthogonal girders (beams of cross sections of 0.3 m×0.7 m or 0.3 m×0.5 m). They support the floor slabs with 0.13 m thickness or the roof slab with 0.1 m thickness. Figure 4 clearly shows that one SNSF cell is made of several RC vertical ribs of 0.11 m thickness with different height (between 0.80 m for the inside ribs up to 2 m for the limit ribs). The hard soil is located 2 m below first floor level. The 2 m excavated soil is used to fill the sub-cells between the ribs and then compacted before carrying out the RC slab to close the cell.

To our knowledge, although well used in the Indonesian construction practice, SNSF foundation

systems have not been studied extensively and considered as a civil engineering research subject. However, the bearing capacity of individual SNSF cells have been the subject of research both numerically and experimentally, see Darjanto (2015), Darjanto *et al. (*2015), Soelarso *et al*. (2019a), El Sawwaf *et al*. (2017).

The present paper deals with a general investigation of the mechanical behavior of SNSF cells in the context of the UNTIRTA project. Part of the paper deals with the static analysis of one cell under vertical loading due to dead and life loads considering symmetry conditions to isolate one cell. In this situation we can compare the behavior of an SNSF cell using the dimensions extracted from the real project with an admissible raft foundation of constant thickness based on Eurocode 2 (2004) or ACI Code 318M-14 (2015). The interaction with of the soft and hard soil is taken into account.

The second part of the paper deals with the evaluation of natural frequencies and mode shapes considering different modeling aspects: one cell of upper-structure, several cells and the whole structure, with and without foundation interaction.

Most of the results have been obtained using advanced FE (finite element) and CAD software from the Altair Hyperworks Platform (like Hypermesh and Optistruct) (https://www.altairhyperworks.com) and also from Autodesk (Revit, Robot Structural Analysis) (https://www.autodesk.com). Different FE models have been established based on 3D beams or 3D solid elements to discretize the upper structure, the SNSF cells and the soil domains. The present study assumes linear isotropic 3D elasticity behavior of the RC structure and the soil (see Bathe 2016, Batoz and Dhatt 1990).

2. Static analysis of SNSF cells with soil interaction under vertical load.

As expressed before, shallow foundation systems based on the replacement of raft slabs by embedded ribs, like the Spider Net System Footing (SNSF) (Figs. 1 to 4) have been the subject of a limited number of papers, see Darjanto *et al. (*2015), Darjanto (2015), Soelarso *et al*. (2019a, b) for example. However, those papers are mainly dealing with the analysis of the load bearing capacity of individual cells based on experimental works or on the finite element modelling using commercial codes. In Soelarso *et al*. (2019a, b) the present authors performed a detailed finite element modelling of a particular cell which was investigated experimentally in Darjanto (2015) and Darjanto *et al.* (2015). Our papers showed a rather good agreement with the experimental results for the displacement under the axial load in the range of linear behaviour of the supporting soil.

The papers by Soelarso *et al*. (2019a, b) also include some comparisons with a raft foundation with uniform thickness designed according to Eurocode 2 (2004) and ACI Code 318M-14 (2015) with respect to punching resistance (see Ahmed *et al*. 2017, Bartolac *et al*. 2015, Fillo *et al*. 2016, Hegger *et al*. 2006).

Based on our experience on the analysis of the bearing capacity of a particular cell we consider the UNTIRTA project described in the introduction and model the cell identified in Fig. 4. The reduced model is shown on Fig. 5.

The cell of dimensions 7 m by 8 m is subjected by a vertical load of 312 tons due to the dead and live loads. The SNSF cell is made of 12 m^3 of RC and the material properties are given in Table 1. For the static analysis we assume symmetry conditions on the vertical planes located at a distance of 4 m in the x direction (u=0) and at 3.5 m in the y direction (v=0). At a depth of 11 m from the slab surface we assume w=0. The 3D FE meshes of one SNSF cell are obtained using Hypermesh (https://www.altairhyperworks.com/). For the results below we consider a mesh of 48268

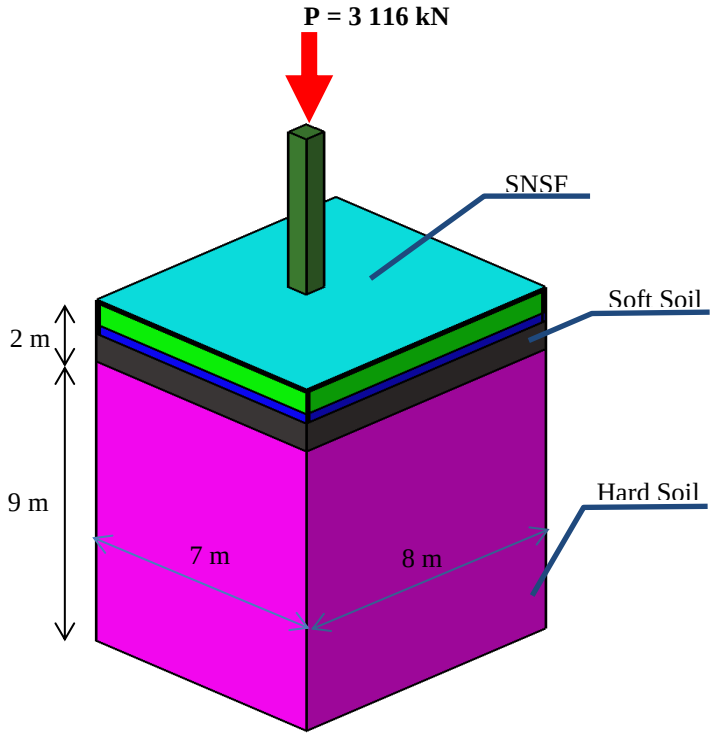

Fig. 5 3D model of the cell including SNSF and supporting soil

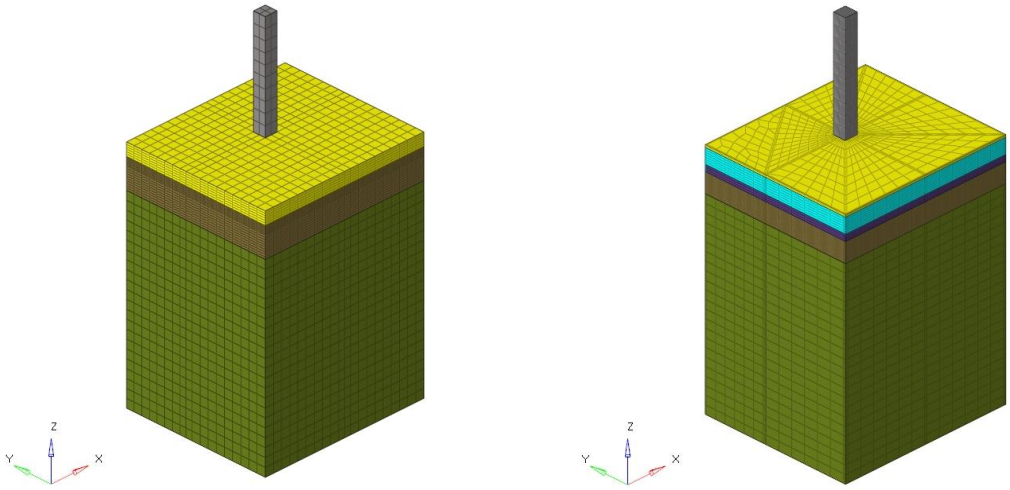

Fig. 6 FE meshes of the raft (left) and SNSF right) structures using H8 elements

Hexahedral elements (with least 2 elements through the thickness of the slab and ribs) involving 148352 dofs. The H8 elements are not classical ones with linear approximations of displacement. They include the incompatible quadratic nodes as proposed by Wilson and Taylor (see Bathe 2016, Batoz and Dhatt 1990). For comparison of results, we model a slab with uniform thickness of 0.6 m

Table 1 Material properties of soil and concrete

Material	Elasticity Modulus (E) (MPa)	Density (T/m^3)	Shear Modulus (G) (MPa)	Poisson
Concrete	21409 (f_c=20 MPa)	2.4	8234	0.2
Soft soil (2 m)	11	1.74	4.6	0.3
Hard soil (9 m)	27	1.75	28.85	0.3

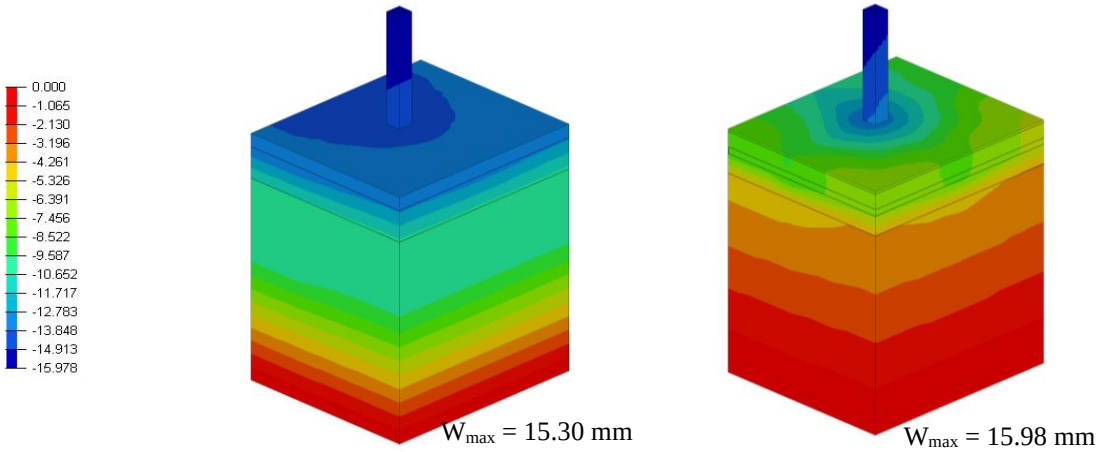

Fig. 7 Vertical displacements for raft (left) and SNSF (right)

(raft) avoiding punching under the vertical load. The FE model is simpler in that case (21596 H8 elements and 67965 dofs) but the volume of concrete is 33.6 m^3 (2.8 times more than for the SNSF). Both finite element 3D meshes are shown on Fig. 6 (including the RC foundation structure and the two layers of soil).

We assume linear homogeneous elastic properties for the concrete and the two types of soil. Full continuity of displacements (sticking contact) is assumed between the soil and the reinforced concrete surfaces, this after a study of the influence of contact conditions on soil-structure surfaces (mainly sliding contact or sticking contact). The results of the linear analysis are compared between the raft and the SNSF systems, using the Optistruct software.

Fig. 7 shows the distribution of the vertical displacements. Both maximum values (around 15 mm) are very close in the two foundation models since the most important contribution of the global elasticity is due to the soil. The raft allows more uniformity of the vertical displacement of the slab surface.

The average compression stress in the column is 8.6 MPa whereas for the soil at 9 m depth it is 0.056 MPa (the allowable bearing capacity from in situ tests is q_{all}=0.2 MPa). The 3D stress distribution in both the raft and SNSF structures are not uniform at all.

On Fig. 8 we show the principal positive stresses (P1) located on both lower surfaces of the raft (left) and SNSF (right). We can clearly see the uniformity of the stress field in the case of the raft whereas the ribs of the SNSF are locally in local severe tension (up to 40 MPa), but in practice, both structures are reinforced by steel rods, according to EC2 or ACI codes. The principal compression stresses P3 are shown on Figs. 9 and 10. The highest compression stresses are acting on the upper slab surfaces: for the raft the max compression stress is found to be -8.9 MPa, whereas for the SNSF the maximum is -22.5 MPa. As a conclusion the SNSF structure appears to be a rather efficient

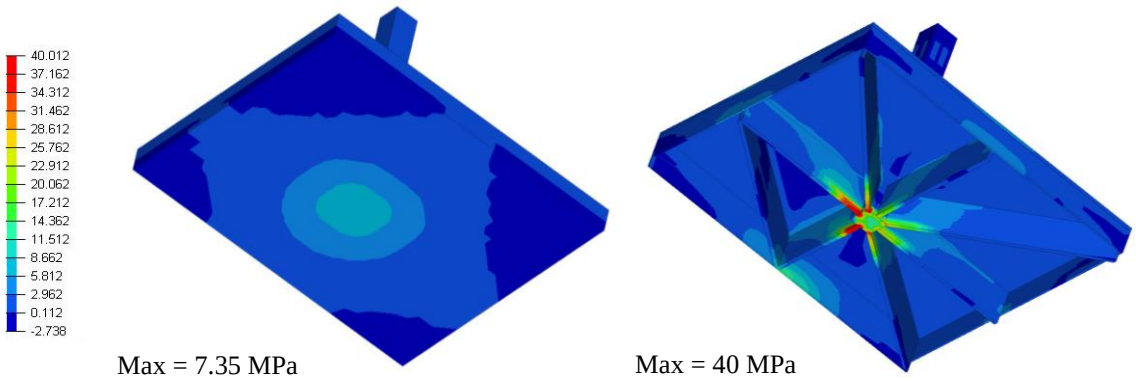

Fig. 8 Distribution of the principal (tensile) stresses P1 for the raft (left) and SNSF (right)

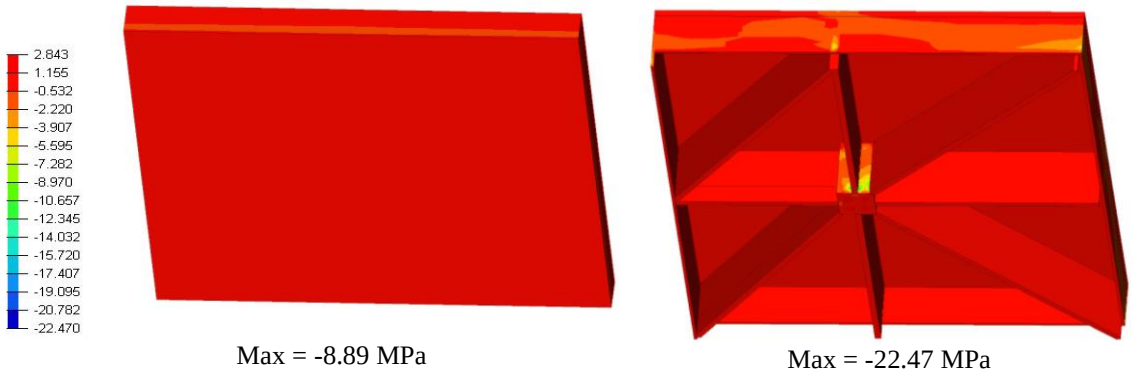

Fig. 9 Distribution of the principal (compression) stresses P3 for the raft (left) and SNSF (right), view from below

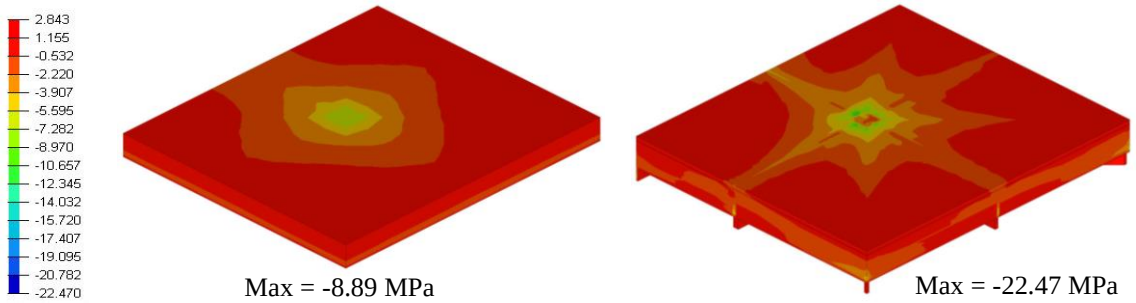

Fig. 10 Distribution of the principal (compression) stresses P3 for the raft (left) and SNSF (right), view from above.

alternative to a classical raft foundation with 280% less reinforced concrete material but for the price of higher cost of manpower. (It was decided to show the principal stresses considering the same scale for both the raft (on left) and the SNSF (on right). This explain some uniformity of colors on Figs. 9 and 10).

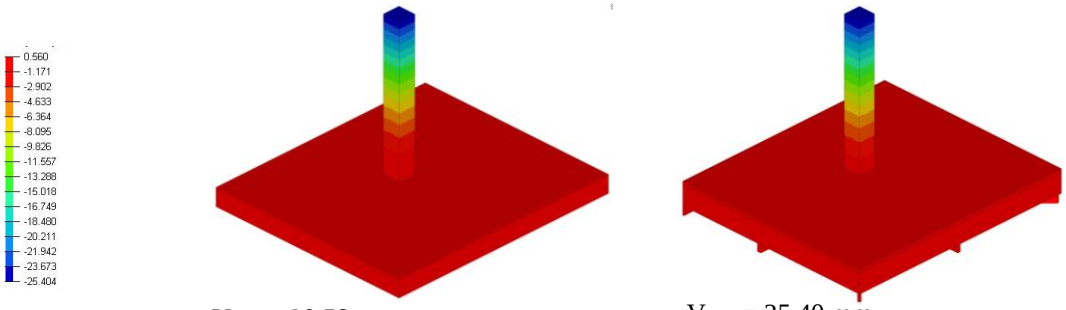

Fig. 11 Displacement fields under the horizontal top force of 10 tons, for the raft (left) and SNSF (right)

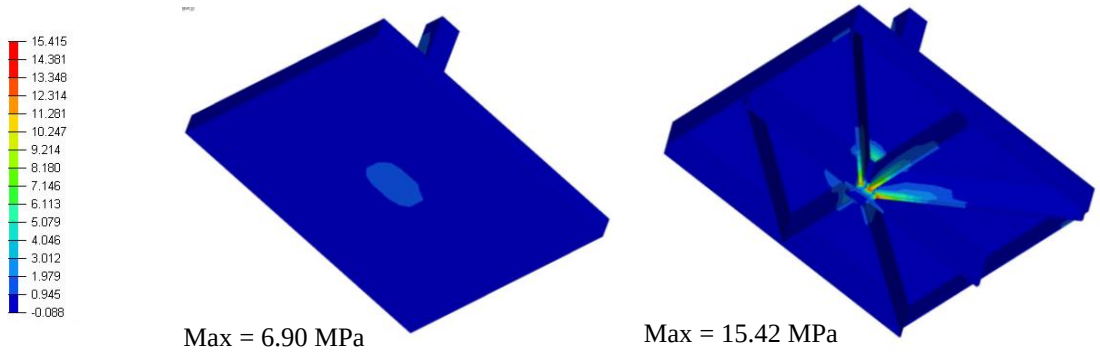

Fig. 12 Distribution of the principal (tensile) stresses P1 for the raft (left) and SNSF (right), under horizontal load

3. Statıc analysıs of the SNSF cell wıth soıl ınteractıon under lateral load.

As buildings in Indonesia are frequently subjected to earthquakes, it is important to analyze and design both the upper structures and their foundations to be earthquake resistant. In order to estimate the behavior of the SNSF system under horizontal loads we perform linear static analyses of the previous isolated SNSF cell and associated raft using FE models as used for the analysis under the vertical load of 312 tons, but we now consider the action of a horizontal load of 10 tons in the y direction (see Fig. 11). With the dimensions of the column (5 m length, square cross section 0.6 m×0.6 m), the horizontal displacement assuming clamping conditions in the slab is equal to (Batoz and Dhatt 1990)

$$v = \frac{P \cdot L^3}{3 \cdot E \cdot I}(1 + \emptyset) = 18.8 \text{ mm}, \qquad \text{with } \emptyset = 0.045 \text{ as the shear influence factor.}$$

The following figures present the results considering the foundation structure and the supporting soil. For the same boundary and symmetry conditions, Fig. 11 shows the displacement field in the y direction (the supporting soil is not represented). It is observed that the SNSF is less stiff compared to a raft (by 9.8%). Also comparing the column with full clamped support (a cantilever beam) and the beam with the SNSF foundation, there is a contribution of 3.9 mm due to the elastic supporting soil and the stiffness of the SNSF.

The bending moment at the base of the column is simply given by $M_x = P \cdot L = 500$ kN. m and the corresponding maximum bending stress is 5.34 MPa. Recalling that under the vertical load

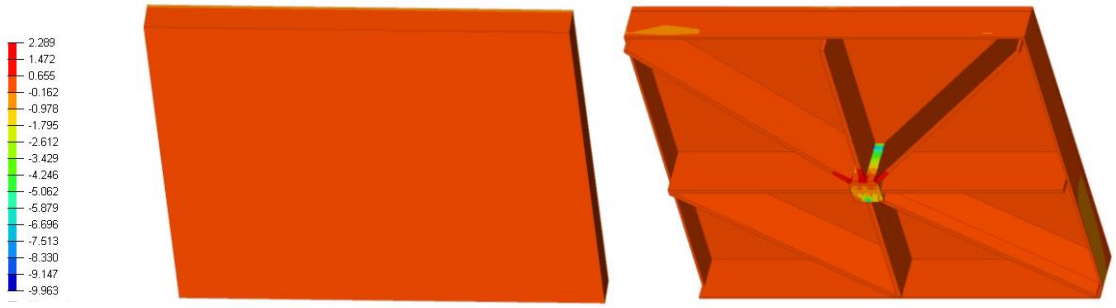

Fig. 13 Distribution of the principal (compression) stresses P3 for the raft (left) and SNSF (right), view from below

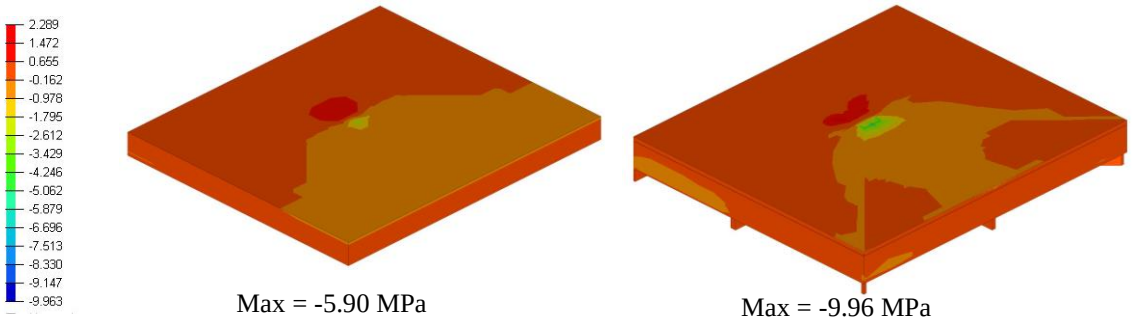

Fig. 14 Distribution of the principal (compression) stresses P3 for the raft (left) and SNSF (right), view from above

of 312 tons, the compression stress is 8.6 MPa we can observe that under the combined action of the vertical force and the horizontal force of 100 kN, the columns will stay in compression at any point of the cross section.

The distribution of the minimum P1 (tensile) stresses is shown on Fig. 12. Again, we can see that the maximum tensile stress is more important in the SNSF (by a factor 2.3) but located in the lowest part of the ribs. Figs. 13 and 14 are related to the distribution of the principal compression stresses and the maximum value is 70% in the SNSF compared to the raft. Those are located in the upper surface of the slab.

To see the influence of the boundary conditions on the four vertical walls, it would be interesting to modify the present model by considering a wider zone of soil around the cells or to consider different boundary conditions on the lateral surfaces of the cell. It would also be necessary to combine the vertical load of 312 tons with the horizontal load of 10 tons in order to have a real picture of the 3D stresses in both structures and locate the maximum tensile and compression stresses.

4. Free vibration analysis with foundation interaction

The next section deals with a first investigation on the role of the shallow foundation system and

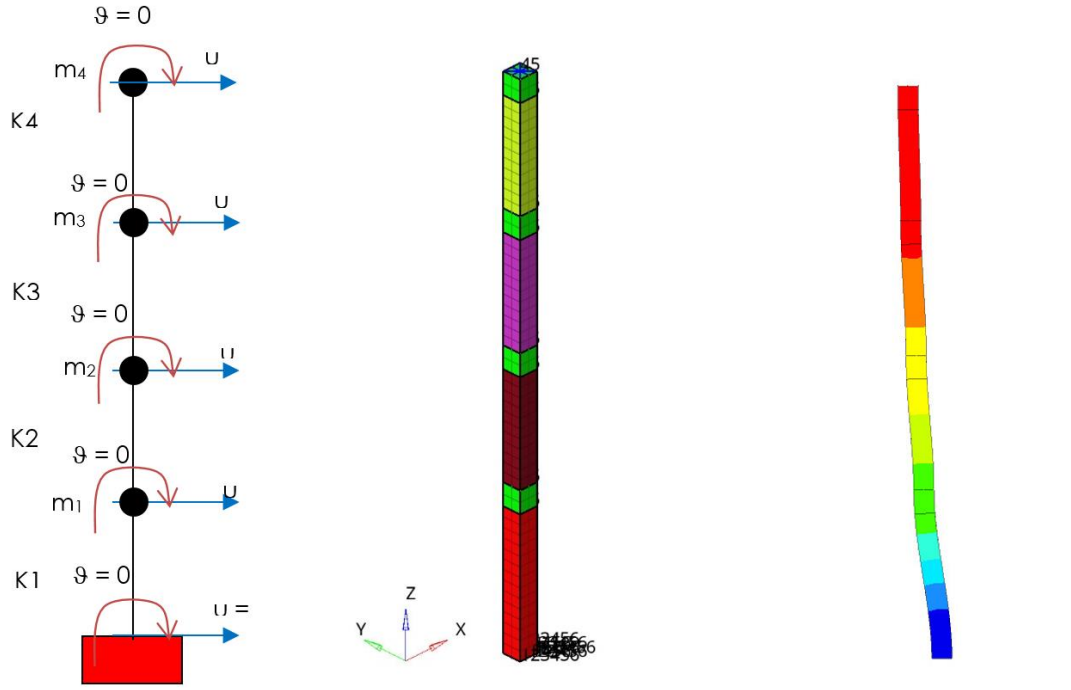

a. 2D beam b. 3D elasticity c. First Mode shape

Fig. 15 2D beam and 3D elasticity models for the free vibration analysis of one column

Table 2 First four frequencies using different 2D and 3D elements for the four floors models

Frequency (Hz)	2D Beam (4 elements)	3D elasticity (Hz)			
		Noe=6315 Dof=25562	Noe=865 Dof=4472	Noe=256 Dof=1685	Noe=208 Dof=1253
f_1	1.043	1.055	1.059	1.066	1.069
f_2	3.183	3.218	3.231	3.255	3.267
f_3	5.202	5.255	5.279	5.319	5.341
f_4	6.658	6.721	6.752	6.804	6.833

*Noe: Number of elements, Dof : Degrees of freedom

underneath soil on the first frequencies and associated mode shapes.

Fig. 15 concerns a first analysis of the free vibration of a single column supporting the four floors and roof. The result is obtained considering a classical 2D beam model using MATLAB. Transverse shear effects are included for the stiffness of one element per column. The concentrated mass on top of each column level is obtained according to the dead and live loads imposed on the upper structure. The total mass is 315 tons (m_1=85 t; m_2=78 t; m_3=78 t; m_4=76 t). At each floor due to the intersection with the girders and slab we assume that the rotation around x or y is zero). Hence there is only one horizontal displacement as dof at each node (Fig. 15, left). The stiffness coefficients Ki are given by (Batoz and Dhatt 1990):

$$K_i = \frac{12EI}{L_i^3(1+\emptyset_i)} \text{ with } \emptyset_i = \frac{12EI}{kGAL_i^2}.$$

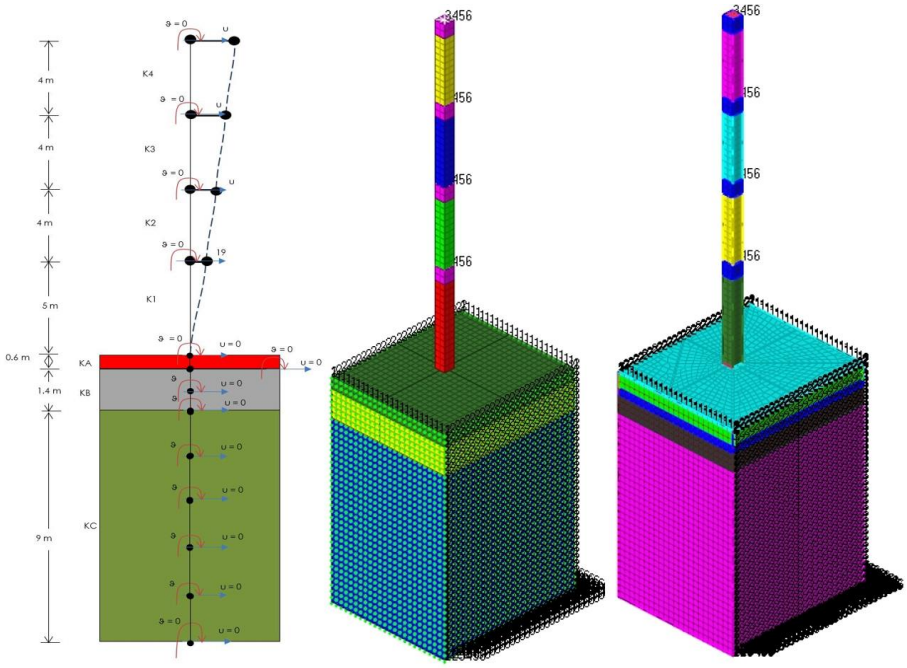

a. 2D beam b. 3D elasticity using raft c. 3D elasticity using SNSF

Fig. 16 2D beam and 3D elasticity models for the free vibration analysis including foundations (raft and SNSF) and soil

We obtain the first frequency as f_1=1.043 Hz. We also build a model (Fig. 15 middle) using Altair Hyperworks based on 3D 6315 H8 elements (25562 dofs). We also constrain the degrees of freedom at each floor intersection (0.7 m) in order to eliminate the rotations around x and y. The result is f_1=1.055 Hz. The first mode shape is shown on Fig. 15 (right).

In Table 2 we report the results for the four first frequencies obtained for the 2D beam model (4 dofs) and the 3D elasticity models for four number of elements. Very similar results are obtained using the 4 elements 2D beam model and the 3D elasticity model with 8 elements per floor in the z direction (last column in Table 2).

In order to evaluate the influence of the foundation and the soil elasticity interactions on the free vibrations we propose the models shown on Fig. 16. On the previous models of Fig. 15(a) and (b) we add the foundations and soil on a domain corresponding to a 8 m×7 m cell and 11 m depth (as in section 2 and 3). As before, we assume symmetry conditions on the four vertical planes. Fig. 16(a) deals with a 2D beam model with several elements in the soil. If the first layer is a raft of 0.6 m depth concrete, then the first four frequencies are the same as in Fig. 15 and Table 2. Fig. 16(b) shows the 3D model considering the four floor levels, a raft of 0.6 m thickness and the two layers of soil (2 m soft soil and 7 m of hard soil). In Fig. 16(c) the raft is replaced by the SNSF structure.

The results (first four frequencies) are given in Tables 3 and 4 considering one cell including either a raft as support or a SNSF. The SNSF model include more elements compared to the raft due to the more complicated geometry but all results are rather similar. There is not much influence of the number of elements in both the raft and the SNSF. The main remark is that the SNSF is slightly less stiff than the raft (f=1.003 for the raft and f=0.984 for the SNSF for the finest 3D meshes).

Table 3 First four frequencies using different 3D elements models for the four floors and soil domain including a raft foundation

Frequency (Hz)	2D Beam	3D elasticity (Hz)		
		Noe = 79 475 Dof = 252 175	Noe = 22 382 Dof = 72 958	Noe = 10 288 Dof = 34 443
f_1	1.043	1.003	1.013	1.018
f_2	3.183	3.160	3.188	3.202
f_3	5.202	5.246	5.287	5.310
f_4	6.658	6.742	6.793	6.822

*Noe: Number of elements, Dof: Degrees of freedom

Table 4 First four frequencies using different 3D elements models for the four floors and a soil domain including one SNSF structure

Frequency (Hz)	2D Beam	3D elasticity (Hz)		
		Noe = 49 744 Dof =151 649	Noe = 27 122 Dof = 85 039	Noe = 17 148 Dof = 53 672
f_1	1.043	0.984	0.970	0.994
f_2	3.183	3.152	3.149	3.197
f_3	5.202	5.270	5.288	5.347
f_4	6.658	6.785	6.814	6.884

*Noe: Number of elements, Dof: Degrees of freedom

Table 5 First four frequencies using 3D elements and a model including the four floors and a soil domain including four piles

Frequency (Hz)	3D Elasticity (Hz)
f_1	0.946
f_2	3.112
f_3	5.270
f_4	6.744

Another model involving one cell is shown on Fig. 17 where the column is supported by four piles of 0.6 m diameter each and 9 m length. The average H8 elements are of size 300 mm resulting in a mesh involving 176 694 elements and 533 905 dofs. The results are given on Table 5. It is seen that the four first frequencies are of the same order of magnitude compared to the SNSF foundation: the deep foundation with four piles leads, for the present model, to a frequency reduction of 4% compared to the shallow SNSF model.

Since the first frequencies obtained with all previous models are very close with the frequencies obtained considering one cell (with constrained boundary conditions), we also explore the influence of the number of cells on the frequency spectrum. With the classical assumption of full clamping at the basis of all columns we evaluate the frequencies for the whole building shown on Fig. 18, using Autodesk Robot (https://www.autodesk.com/). That analysis is based on 3D beam elements and for the contribution of the mass, both the dead loads of the upper structure and the live loads applied of the floor slabs are taken into account. The model is shown on Fig. 18 together with a view of the first mode. The last model presented in this paper involves a part of the structure. The first frequency

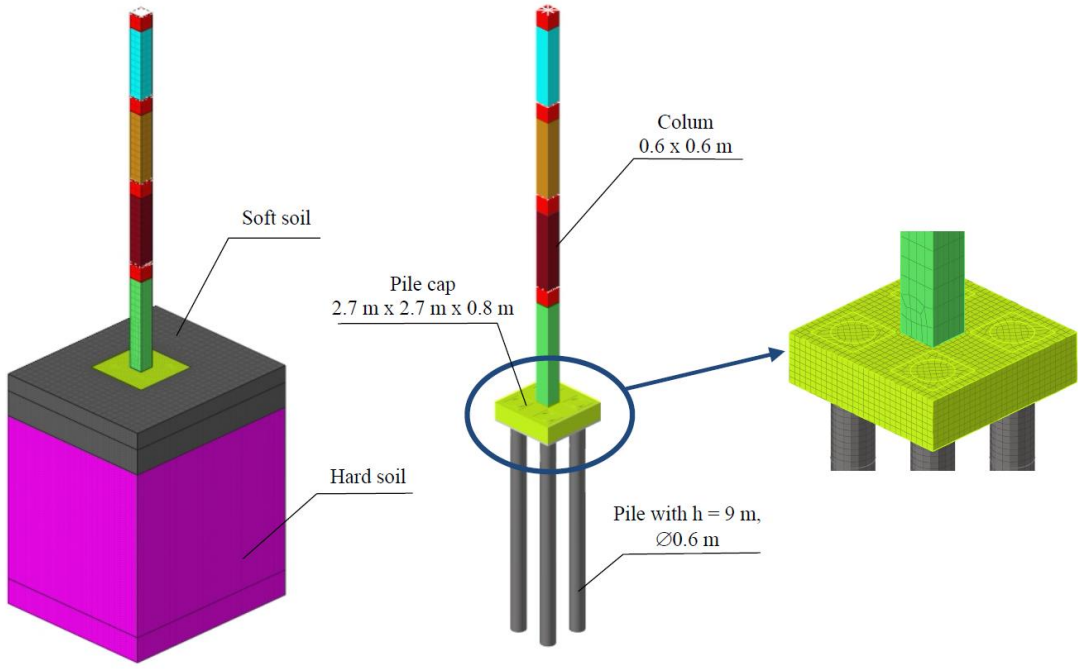

Fig. 17 Model of one cell with a four floors column supported by four piles

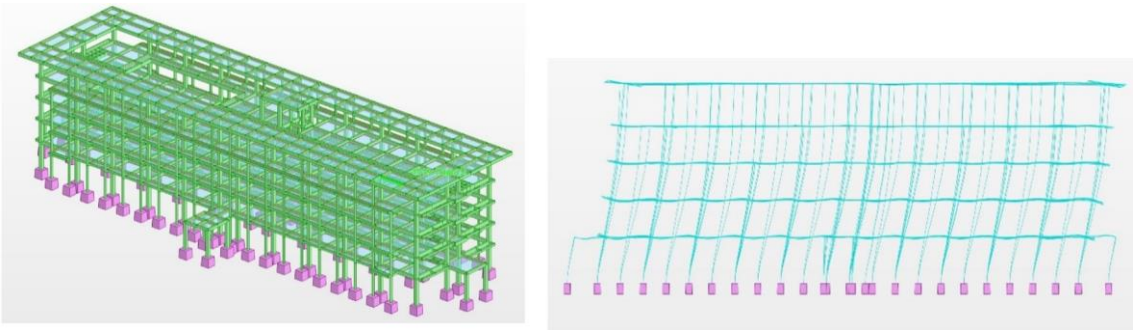

(a) 3D beam (b) Mode shape

Fig. 18 Modal analysis of the full building using Autodesk Robot

for the whole building (Fig. 18) is equal to 0.97 Hz whereas it is equal to 0.96 Hz for the selected part of the building (Fig. 19). Hence, we can conclude that the first frequency around one Hz is quite independent of the size of the model of the structure without foundation and supporting soil. Therefore, we can continue to focus on a single cell in order to study the behavior of the shallow foundation (in particular of the SNSF type).

4. Conclusions

The paper deals with RC buildings of 5 to 8 floors supported by a shallow foundation system

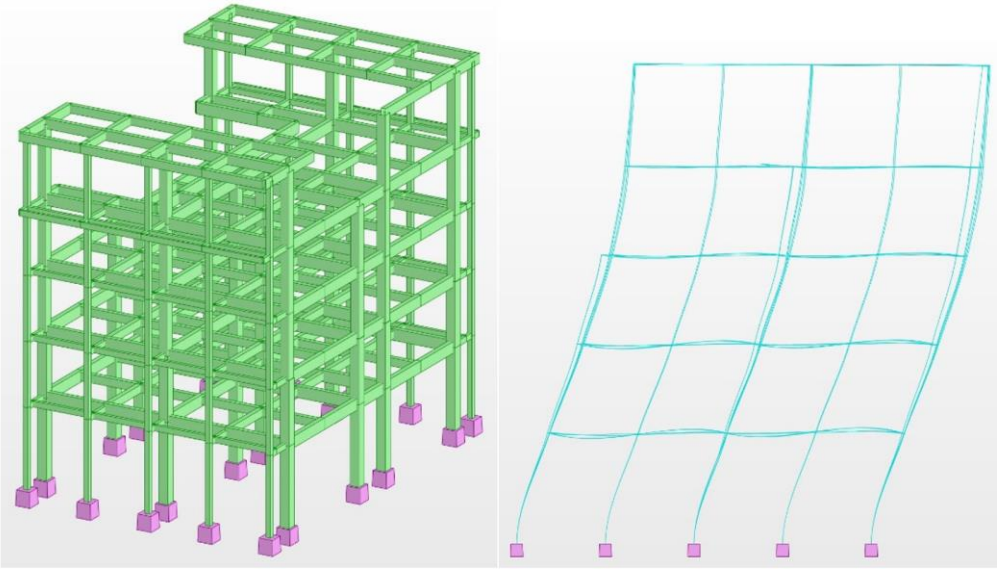

(a) 3D beam (b) Mode shape

Fig. 19 Modal analysis of part of the complete building using Autodesk Robot

called SNSF (Spider Net System Footing), often used in Indonesia in poor soil conditions. SNSF is composed of continuous cells made of vertical ribs in different directions and heights. The columns are located at the center. The cavities between the ribs are filled with soil and those are then closed by a RC slab. The present paper is a contribution to the structural analysis of that type of shallow foundation. We propose a detailed structural linear analysis of one cell with one column subjected to a concentrated vertical load, taking into account the elastic behavior of the soil inside the cell and the different layers of soil under the cell. Symmetry conditions are taken into account on the boundary of the cell. To better characterize one SNSF cell we compare the results with those obtained for a uniform thickness slab designed to avoid punching under the column (but involving around three times more concrete!). In a second part we consider the action of a lateral load on top of the 5 m height column (first floor). The static load is "equivalent" to a small dynamic load.

The SNSF appears to be less stiff than the raft but the order of stiffness is the same. The maximum stresses appear also acceptable and compatible with reinforced concrete design. However detailed analyses are still needed to evaluate the stress fields when vertical and lateral loads are combined. The last part of the paper shows that the first four frequencies are almost independent of the models we consider: 1) 2D beam for four floors or 3D elasticity with H8 elements with clamping conditions at the basis, 2) one cell modeled with 2D beams with soil, one cell with a column plus a raft and soil, one cell with a column plus a SNSF structure and the soil underneath and also one cell with a column supported by four piles of 11 m length. The first frequency is always found around one Hertz. It seems also that there is no much influence of the number of cells taken into account (same results for the model of the complete building or for a part of it).

Further investigations are needed to better characterize the SNSF structures in both static and dynamic conditions. It is also interesting to do additional research on the optimal design of such SNSF structures taking into account the mechanical as well as the practical economy aspects.

Acknowledgements

The present study is part of the Ph.D thesis prepared by the first author. The scholarship provided by the Islamic Bank of Development for the UNTIRTA project "food security" is duly acknowledged.

References

ACI Code 318M-14 (2015), Building Code Requirements for Structural Concrete, American Concrete Institute.

Ahmed, F.R., Hamad, K.K. and Rashied, Z.N. (2017), "Prediction of punching strength of reinforced concrete footings by finite element method", *Am. J. Civil Eng. Arch.*, **5**(1), 8-16. https://doi.org/10.12691/AJCEA-5-1-2.

Al-Aghbari, M.Y. (2007), "Settlement of shallow circular foundations with structural skirts resting on sand", *J. Eng. Res.*, **4**(1), 11-16. https://doi.org/10.24200/tjer.vol4iss1pp11-16.

Bartolac, M., Damjanović, D. and Duvnjak, I. (2015), "Punching strength of flat slabs with and without shear reinforcement", *Gradjevinar*, **67**(8), 771-786. https://doi.org/10.14256/JCE.1361.2015.

Bathe, K.J. (2016), *Finite Element Procedures*, Prentice Hall, Pearson Education, Inc.

Batoz, J.L. and Dhatt, G. (1990), *Modélisation des Structures par Élément Finis, Volume 1 : Solides Elastiques*, Hermes Science Publication/Lavoisier, France.

Batoz, J.L. and Dhatt, G. (1990), *Modélisation des Structures par Éléments Finis, Volume 2 : Poutres et Plaques*, Hermés Science Publications/Lavoisier, France.

Darjanto, H. (2015), "Load transfer mechanisms in the cell spider net system footing construction through full-scale static and cyclical vertical loads and 3d numerical analysis", Ph.D. Dissertation, Diponegoro University, Semarang, Indonesia.

Darjanto, H., Irsyam, M. and Retno, S.R. (2015), "Full scale load test on the spider net system", *Jurnal Teknologi (Sciences & Engineering). Universiti Teknologi Malaysia*, **77**(11), 73-82.

El Sawwaf, M., Nazir, A., Azzam, W. and Mohy, A. (2017), "Utilization of embedded ribs for improving the bearing capacity of raft foundation in sand", *International Conference on Advances in Structural and Geotechnical Engineering*, Hurghada, Egypt, April.

Eurocode 2, (2004), Design of Concrete Structure, Eurocode Standards.

Fillo, Ľ., Augustín, T., Knapcová, V. and Labudková, J. (2016), "Influence of footings stiffness on punching resistance", *Perspect. Sci.*, **7,** 204-207. https://doi.org/10.1016/j.pisc.2015.11.034.

https://www.autodesk.com/

https://www.katama.co.id/

Hegger, J., Ricker, M., Ulke, B. and Ziegler, M. (2007), "Investigations on the punching behaviour of reinforced concrete footings", *Eng. Struct.*, **29**(9), 2233-2241. https://doi.org/10.1016/j.engstruct.2006.11.012.

Ibrahimbegovic, A. (2009), *Nonlinear Solid Mechanics: Theoretical Formulations and Finite Element Solution Methods*, Springer, Berlin.

Paz, M. (1985), *Structural Dynamics: Theory and Computation*, 2nd Edition, Springer, New York.

Ponginan, R. (2018), *Learn Dynamic Analysis with Altair OptiStruct*, 2nd Edition, Altair University.

Soelarso, S., Antaluca, E., Batoz, J.L. and Lamarque, F. (2019), "On the finite element bearing capacity analysis of a rib system to be used as shallow foundation construction", *Best Conference Proceedings*, Bali, August.

Soelarso, S., Antaluca, E., Batoz, J.L. and Lamarque, F. (2019), "On the finite element modeling and bearing capacity of two shallow foundation systems", Université de Technologie de Compiègne, Internal Research Report.